Microbial population dynamics and evolutionary outcomes under extreme energy limitation

William R. Shoemaker[a,b,1], Stuart E. Jones[c], Mario E. Muscarella[a,2,3], Megan G. Behringer[a,4], Brent K. Lehmkuhl[a], and Jay T. Lennon[a,1]

[a]Department of Biology, Indiana University, Bloomington, IN, 47405; [b]Department of Ecology and Evolutionary Biology, University of California, Los Angeles, CA 90095; and [c]Department of Biological Sciences, University of Notre Dame, Notre Dame, IN 46556

Edited by Richard E. Lenski, Michigan State University, East Lansing, MI, and approved July 8, 2021 (received for review January 27, 2021)

Microorganisms commonly inhabit energy-limited ecosystems where cellular maintenance and reproduction is highly constrained. To gain insight into how individuals persist under such conditions, we derived demographic parameters from a collection of 21 heterotrophic bacterial taxa by censusing 100 populations in an effectively closed system for 1,000 d. All but one taxon survived prolonged resource scarcity, yielding estimated times to extinction ranging over four orders of magnitude from 10^0 to 10^5 y. Our findings corroborate reports of long-lived bacteria recovered from ancient environmental samples, while providing insight into mechanisms of persistence. As death rates declined over time, lifespan was extended through the scavenging of dead cells. Although reproduction was suppressed in the absence of exogenous resources, populations continued to evolve. Hundreds of mutations were acquired, contributing to genome-wide signatures of purifying selection as well as molecular signals of adaptation. Consistent ecological and evolutionary dynamics indicate that distantly related bacteria respond to energy limitation in a similar and predictable manner, which likely contributes to the stability and robustness of microbial life.

longevity | microbial ecology | life history | necromass | molecular evolution

Microorganisms are the most abundant and diverse group of organisms on the planet. Their metabolic repertoire and capacity for rapid reproduction across environmental conditions help catalyze and regulate the biogeochemical processes that sustain life on Earth. Yet, microorganisms are often challenged by energy supplies that barely meet their basal metabolic demands (1–5). As a result, many microorganisms in nature rest on the cusp of life and death (1, 6–9). For example, more than half of the microbial cells in the global ocean reside in deep sediments or underneath continental plates where exploitable energy is vanishingly small (10). In permafrost-dominated ecosystems, which cover roughly 25% of Earth's surface (11), microorganisms must survive for extended periods of time between freeze-thaw events before reproduction is favorable (12). Even in the mammalian gut, which is commonly viewed as a resource-rich environment, microorganisms must tolerate feast-or-famine conditions if they are to survive passage and colonize new hosts (13). Despite being recognized as a universal constraint, the ecological and evolutionary dynamics that emerge under thermodynamically unfavorable conditions are rarely examined. Identifying the mechanisms by which energy limitation affects microbial populations has the potential to reshape our understanding of microbiomes in environmental, engineered, and host-associated ecosystems.

Across the tree of life, organisms are confronted with how to best allocate energy in order to maintain homeostasis when resources are scarce. Microorganisms have evolved a wide array of traits that can extend their lifespan and maximize fitness in energy-limited environments (3, 14). While some taxa have the flexibility to generate ATP using different combinations of electron acceptors and electron donors, other organisms are specialized in the assimilation of unique substrates or the conservation of energy by temporarily suspending their metabolic activities (15–19). Ultimately, variation in such strategies contributes to the assembly of complex communities, but the degree to which functional traits extend the lifespan of a typical microorganism is relatively unknown, even though energy limitation has important implications for the diversity, stability, and persistence of microbial systems (17, 20–23).

When energy inputs approach zero, habitats can take on the properties of a closed system (24). This limit occurs when the residence time of a system is extremely long, a characteristic that commonly arises in disparate environments, including lakes, soils, and glaciers (25–28). Under such conditions, dispersal is restricted and resource supply rates are governed by endogenous dynamics that involve the internal recycling of materials and energy (29–31). For example, dead cells can be scavenged by surviving individuals to meet their maintenance requirements and support limited cellular division (32). However, the extent

Significance

Energy limitation is a widespread phenomenon that governs microbial processes ranging from the metabolism of individual cells to the functioning of the biosphere. By tracking the population dynamics of diverse bacterial taxa under prolonged starvation, we identified common strategies that sustain life. Although bacteria have the capacity to reproduce on timescales of minutes to hours, we predict that populations can persist for hundreds to thousands of years, placing upper bounds on microbial lifespans. While the dynamics observed in our long-term experiment were driven by a reduction in death rates, cryptic birth events generated mutations that fueled evolution. Our findings shed light on cellular longevity with implications for biodiversity in extreme environments that dominate vast expanses of Earth.

Author contributions: W.R.S., S.E.J., B.K.L., and J.T.L. designed research; W.R.S., M.E.M., and B.K.L. performed research; W.R.S., M.G.B., and B.K.L. contributed new reagents/analytic tools; W.R.S., S.E.J., and M.G.B. analyzed data; and W.R.S., S.E.J., M.E.M., M.G.B., B.K.L., and J.T.L. wrote the paper.

The authors declare no competing interest.

This article is a PNAS Direct Submission.

See online for related content such as Commentaries.

[1]To whom correspondence may be addressed. Email: williamrshoemaker@gmail.com or lennonj@iu.edu.

[2]Present address: Institute of Arctic Biology, University of Alaska Fairbanks, Fairbanks, AK 99775.

[3]Present address: Department of Biology and Wildlife, University of Alaska Fairbanks, Fairbanks, AK 99775.

[4]Present address: Department of Biological Sciences, Vanderbilt University, Nashville, TN 37232.

This article contains supporting information online at https://www.pnas.org/lookup/suppl/doi:10.1073/pnas.2101691118/-/DCSupplemental.

Published August 12, 2021.

to which necromass recycling can sustain biological systems is unclear. Demographic properties such as population size, along with birth and death processes, dictate the size and flux of the necromass pool. Ultimately, this internally generated resource will diminish over time because the amount of exploitable energy released by a dead cell is less than the amount of energy required to build a new cell (33). Fundamentally, these thermodynamic constraints place hard limits on the persistence and evolution of populations in an effectively closed system. Nevertheless, genetic and phenotypic changes arise in model organisms when they are exposed to prolonged starvation under laboratory conditions, a phenomenon known as growth advantage in stationary phase (34–40). Similar observations have been made in natural environments. Selection at the molecular level has been documented in the deep biosphere where microbial biomass in the marine subsurface turns over on a timescale of hundreds to thousands of years, owing to extreme energy limitation (41). Yet in other instances, energy-limited bacteria have been reported to be evolutionarily static over geologic timescales (42).

Using a combination of comparative and experimental approaches, we characterized the ecological and evolutionary dynamics of energy-limited bacteria. We conducted survival analyses on 100 populations belonging to 21 bacterial taxa in an effectively closed system with zero resource inputs over 1,000 d. We assessed variation in key demographic parameters, with an emphasis on how necromass recycling alters the net population growth rate using metabolomics, functional traits, dynamical models, single-cell metabolic assays, and estimates of cellular division. Genetic manipulations allowed us to quantify how protective structures (endospores) affect cellular lifespan and the time to extinction for energy-limited populations. Last, we evaluated the extent to which bacteria evolve under energy limitation by quantifying the frequency of de novo mutations and the strength of purifying selection while testing for signatures of adaptation at the molecular level. Together, this multifaceted approach allowed us to identify the predictable ways in which phylogenetically diverse taxa survive and evolve in energy-limited environments.

Results and Discussion

Over the course of 1,000 d, nearly all bacterial populations survived conditions of extreme energy limitation. Using the Weibull distribution, we determined that the net population growth rate (births – deaths) increased over time, a pattern exhibited by all but one taxon (Fig. 1). We identified a strong inverse relationship between the initial flux of cell death ($d_0 \cdot N(0)$) and the change in the net population growth rate (k) (Fig. 2), consistent with the interpretation that starved cells can meet their maintenance energy requirements through necromass recycling. Multiple lines of evidence support the view that these changes in net population growth rate were driven by a decrease in death rates. Based on this information, we derived estimates of longevity as the mean time to death of a cell ($\bar{T}_d \sim 10^0$ to 10^3 d) and the mean time to extinction of a population ($T_{ext} \sim 10^0$ to 10^5 y) (Fig. 2), which we put into context with literature-reported estimates for plant and animal species. Although extreme energy limitation placed constraints on metabolism and reproduction, pooled sequencing revealed signatures of purifying selection and adaptation, which taken together provide insight into the ecology and evolution of populations in a closed system.

Net Population Growth Rates Increase over Time under Energy Limitation. We tracked the density of nearly 100 populations belonging to a diverse collection of chemoorganoheterotrophic bacteria

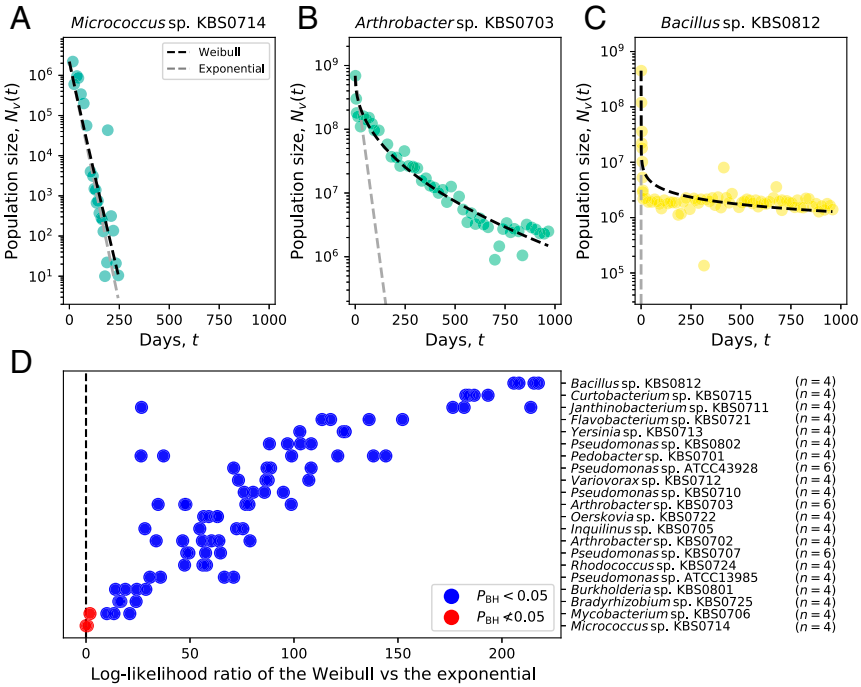

Fig. 1. The shape of the survival curves was highly variable among energy-limited bacterial taxa maintained in an effectively closed system. The rate of decay for *Micrococcus* sp. KBS0714 (*A*) was near-linear on a semilog scale, indicating that the net population growth rate did not change with time ($k = 0.96 \approx 1$). In contrast, the survival curves of *Arthrobacter* sp. KBS0703 (*B*) and *Bacillus* sp. KBS0812 (*C*) exhibited clear curvature, meaning that the net population growth rate increased over time (*D*). We used maximum likelihood while correcting for false discovery rate ($\alpha = 0.05$) to formally compare survivorship with (Weibull) and without (exponential) curvature. With the exception of *Micrococcus* sp. KBS0714, the survival curves for all taxa were best fit by the Weibull distribution. Across taxa, there was no phylogenetic signal associated with the survival-curve parameters (*Materials and Methods* and *SI Appendix*, Fig. S10) ($LR = 7.6$, $\lambda_{Pagel} \approx 0$, $P = 0.009$).

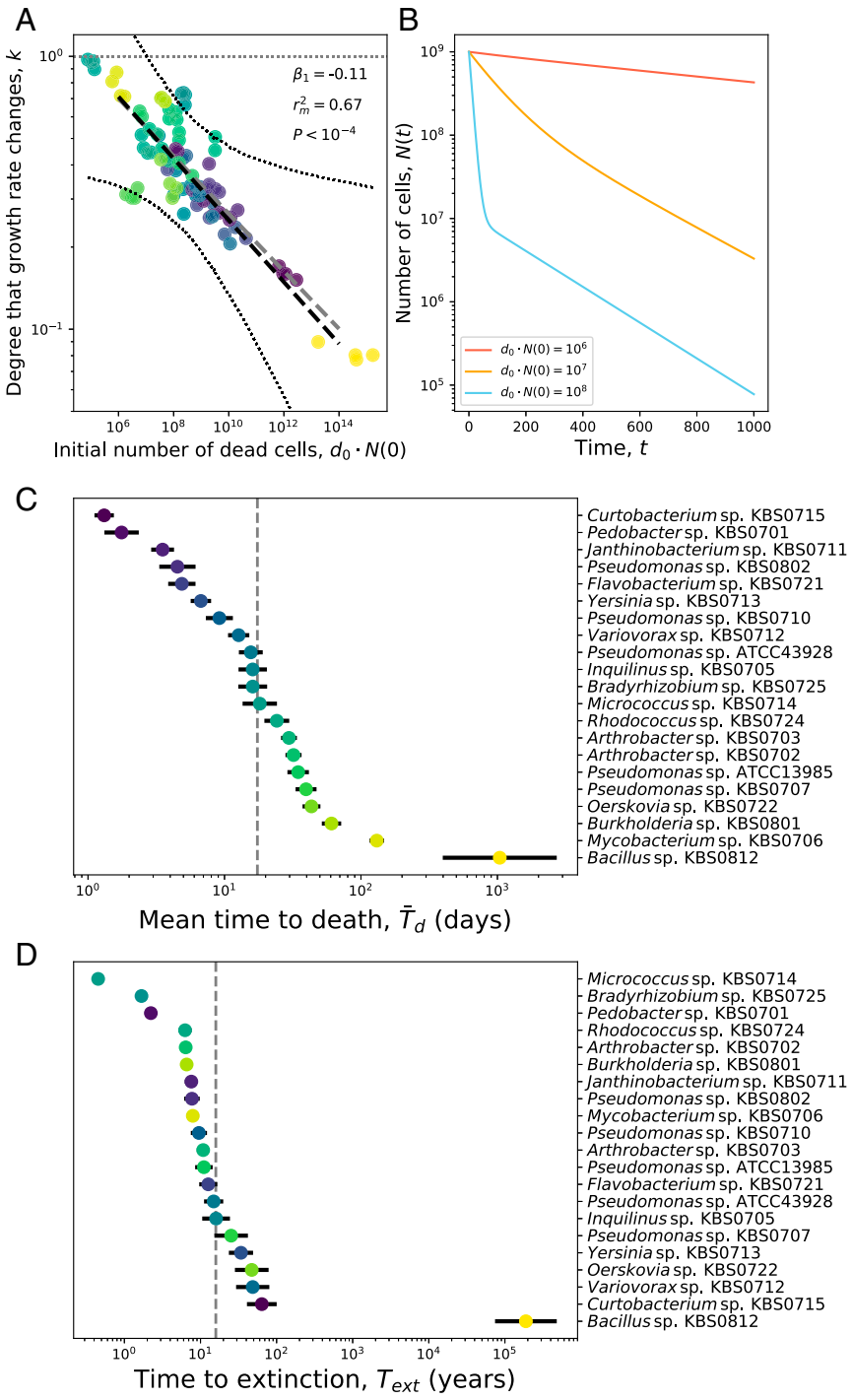

Fig. 2. (*A*) Populations with more deaths [larger $d_0 \cdot N(0)$] had a larger increase in the net population growth rate over time (smaller k), a finding that is consistent with predictions based on the necromass recycling hypothesis (Eq. **2**), illustrated in *B*. (*C* and *D*) Using these demographic parameters, we examined the mean time to death ($\bar{T}_d$) and the time to extinction (T_{ext}). In *A*, long-dashed black and gray lines represent predicted values from the fixed effect and phylogenetic regressions, respectively. The dotted black lines represent 95% confidence hulls, while the horizontal dotted gray line represents the value of k if the net population growth rate did not change over time, which would be expected if the survivorship curves followed a negative exponential relationship. Black bars in *C* represent twice the SE, and the gray vertical dashed line represents the mean across all taxa.

(*SI Appendix*, Table S1) that were maintained under controlled conditions in a pH-buffered solution without an external supply of electron donors. Although samples were taken over time for population censusing via colony-forming unit (CFU) counts, this had minimal effect on the volume and headspace of the experimental units (*Materials and Methods*). As such, we interpret the ecological and evolutionary dynamics as having emerged in an effectively closed system.

With the resulting time series, we performed survival analyses using the Weibull distribution (Eq. **1**). This model is commonly used in engineering, sociology, and manufacturing to characterize the reliability of a system by estimating the amount of

time until an event takes place (43). Demographers also use the Weibull distribution to describe patterns and elucidate the underlying processes that contribute to population dynamics. In addition to the scale parameter d_0, which estimates the initial per-capita death rate, the Weibull generates a shape parameter k that characterizes how populations change over time. For example, when $k = 1$, a constant fraction of individuals is lost at each time step, resulting in a first-order survivorship curve that appears linear on a semilogarithmic plot. When $k > 1$, the survivorship curve accelerates, a phenomenon this often associated with the wear-out of a device or the senescence of aging individuals. Last, survivorship curves can take on a decelerating form ($k < 1$), indicating that the net population growth rate increases over time, due to either more births or fewer deaths.

Nearly all of the survival curves deviated from first-order decay. Although a deceleration in survivorship has previously been observed (44–46), a comparative investigation of this pattern with diverse taxa over an extended period of time has not been conducted. For more than 90% of the energy-limited populations, we observed that $k < 1$, meaning that net population growth rates (births − deaths) increased over time (Fig. 1 and *SI Appendix*, Figs. S1–S3). Model comparison based on likelihood ratios confirmed that the Weibull distribution best explained the survival curves for all except one taxon. In contrast to other bacteria, survivorship for *Micrococcus* sp. KBS0714 was best explained by an exponential model ($k = 1$). It is worth noting that all replicate populations belonging to this taxon went extinct by day 300 (Fig. 1*D*).

Although the Weibull was generally very effective at fitting our survivorship data, we explored other models that might provide insight into the population dynamics of energy-limited microorganisms. For example, the Gompertz model has been used to describe the dynamics of plant and animal populations (47), but it performed poorly with our data. We also considered that a decelerating survivorship might reflect phenotypic heterogeneity within a bacterial population. However, the Weibull consistently outperformed a biexponential model that incorporated mortality rates for different cell types (*SI Appendix*, Fig. S4). Therefore, in the following sections, we explore how an internally generated resource (necromass) contributed to changes in the net population growth rates of bacteria in an effectively closed system.

Cellular Recycling Likely Sustained Energy-Limited Populations. Given the prevalence of the demographic pattern across taxa, we sought a common explanation for the curved form ($k < 1$) of the survivorship data. In an effectively closed system, we hypothesized that microorganisms meet their maintenance energy requirements and generate new biomass by consuming the one resource that can accumulate over time: necromass. We assumed that the initial flux of necromass (R) into the system was proportional to the initial number of cellular deaths, defined here as the initial number of cells times the initial per-capita death rate [$\partial R_t \propto d_0 \cdot N(0)$]. Based on this logic, if an increase in the net population growth rate was due to viable cells scavenging dead cells for energy, then we would expect k to decrease as the initial number of dead cells increased. We found that this was the case, based on the strong inverse relationship between the two variables ($t_{19} = -7.85$, $r^2 = 0.67$, $P < 10^{-5}$) (Fig. 2*A*), which was also robust at the taxon level based on the results from a mixed model analysis. The linear relationship also provides a compelling explanation for why *Micrococcus* sp. KBS0714, the taxon with smallest $d_0 \cdot N(0)$, consistently went extinct.

To further investigate the necromass recycling hypothesis, we characterized the fate of dead cells in our populations. Based on single-cell metabolic assays, the change in the proportion of dead cells varied across taxa, but it was nowhere near the expected value of ~ 1 if dead cells had accumulated over 1,000 d (*Materials and Methods* and *SI Appendix*, Fig. S5). The lack of dead cells suggested that substantial decomposition occurred over the course of the experiment. As expected, concentrations of cellular components in the dissolved fraction of the populations were very low. Metabolites at day 1,000 were undetectable for all five taxa examined (*SI Appendix*, Fig. S6), and amino acid levels were below the mass spectrometer detection limits for *Bacillus* (*SI Appendix*, Fig. S7). Given that the number of cell deaths after 1,000 d exceeded 10^9 ($\sim 10^8$/mL), our data are consistent with the interpretation that the surviving cells consumed appreciable quantities of necromass.

Other lines of evidence lend additional support to the necromass recycling hypothesis. We documented a strong relationship between k and lag time, which reflects the amount of time it takes for a population to enter an exponential growth phase under energy-replete conditions ($t_{19} = 3.38$, $r^2 = 0.37$, $P = 0.0.0013$) (*SI Appendix*, Fig. S8). This pattern suggests that populations benefiting from necromass consumption also have a shorter lag time. Such an outcome is predicted by kinetic models of cellular reproduction, where lag time increases if cells lack sufficient resources to maintain autocatalytic processes (48–50). Last, we were able to reproduce empirical trends from our survival analysis using a simple dynamical model that allowed for changes in the net population growth rate as a consequence of necromass uptake according to Monod kinetics (Eq. **2** and Fig. 2*B*).

Reduced Death Rates Likely Increased Net Population Growth. While massive cell die-off dominated the early phase of our experiment, survival curves alone cannot determine whether demographic changes over time were due to a decrease in death rate or an increase in birth rate. It is very difficult to quantify birth rates in energy-limited populations that are out of equilibrium with a low net population growth rate. Therefore, we used the index of replication (iRep), a sequence-based proxy of birth rate where a value of 1 indicates that no cells were reproducing, whereas a value of 2 indicates that all cells were dividing (51). This approach revealed that on average, 50% ($\overline{\text{iRep}} = 1.49$) of the energy-limited bacteria were reproducing on day 1,000. However, there was no statistically significant relationship between iRep values and k (*SI Appendix*, Fig. S9) ($t_{13} = 0.69$, $r^2 = 0.036$, $P = 0.500$), suggesting that birth rate alone was insufficient to drive the increase in the net population growth rate. Moreover, there was no relationship between k and the maximum growth rate ($\mu_{\max}$, approximately equal to the maximum birth rate) in energy-replete environments, which we would expect if an increase in the net population growth rate was primarily driven by a large increase in birth rate. Last, the fact that no de novo mutations fixed over 1,000 d in any population indicates that very few generations occurred during our experiment. Taken together, the number of estimated birth events was insufficient to explain the observed increase in the net population growth over time.

Although variation in k was primarily due to decreasing death rates, our study provides insight into the birth dynamics of populations in an effectively closed system. When biomass was sufficient, we performed pooled population sequencing to obtain estimates for the maximum size of a mutant lineage [$f_{\max} \cdot N(1,000) \approx N_{mut}$; Table 1] by multiplying the maximum frequency of all de novo mutations by the final population size at day 1,000. Because $\gtrsim 95\%$ of mutations were unique to a given population, we can safely assume that the majority of mutant lineages within a population arose after the initial culture was split into replicates (*Materials and Methods*). If lineages subsequently increased in size according to a pure birth branching process, the number of generations required to create a lineage of size N_{mut} is $\log_2(N_{mut})$. Accordingly, we calculated a mean

Table 1. Demographic estimates inferred from sequence data across taxa

Taxon	n_{mut}	$\bar{f}$	$f_{\max}$	$b_{\min}$	T_2 days	$b_{\min}/N(1,000)$
Pseudomonas sp. ATCC13985	208	0.14	0.64	7.30×10^5	50	0.30
Arthrobacter sp. KBS0702	359	0.078	0.34	1.30×10^5	65	0.12
Curtobacterium sp. KBS0715	79.3	0.14	0.56	1.20×10^5	66	0.20
Flavobacterium sp. KBS0721	53.2	0.13	0.40	4.90×10^4	75	0.14
Oerskovia sp. KBS0722	79.3	0.098	0.45	1.60×10^6	53	0.17
Rhodococcus sp. KBS0724	53.0	0.11	0.32	8.90×10^4	69	0.088
Burkholderia sp. KBS0801	29.0	0.14	0.41	5.50×10^5	55	0.15

The terms $\bar{f}$ and $f_{\max}$ represent the mean and maximum observed mutation frequency calculated from a mean of n_{mut} mutations in a population, respectively. The term $b_{\min}$ is the minimum number of cell divisions as a binary branching process calculated from $f_{\max}$. T_2 is the mean time to cell division using $b_{\min}$, and $b_{\min}/N(1,000)$ is the percent that birth events contributed to the curvature at day 1,000.

generation time of $(\log_2(N_{mut})/1,000\ d)^{-1} \approx 60-75$ d, which is three orders of magnitude larger than the doubling time measured under energy-replete conditions (52). Continuing with the branching process assumption, we calculated the minimum number of birth events ($b_{\min}$) necessary to generate N_{mut} individuals and compared that estimate to $N(1,000)$ with and without the survivorship curvature (k), which allowed us to arrive at an estimate for the contribution of birth events to the increase in $N(t)$ over time. Because virtually all populations declined by several orders of magnitude in the first 100 d, the number of individuals at day 1,000 would be zero if the net population growth rate did not increase over time. This observation allowed us to estimate the minimum contribution of births to the difference in $N(1,000)$ if the net population growth rate did not increase over time, resulting in a range of $\frac{b_{\min}}{N(1,000)} \approx 0.08$ to 0.3 (Table 1). While this calculation is admittedly coarse, it bolsters the claim that births cannot be the dominant demographic force in our study.

Longevity and Extinction Were Taxon Specific. Given that energy-limited population dynamics were driven by a decrease in death rates, we were able to use the Weibull parameters to estimate the lifespan of a cell. We found that the mean time until death $\bar{T}_d$ ranged from $\sim 10^0$ to 10^2 d (Fig. 2*C*), with a mean $\bar{T}_d$ among all taxa of $\sim$17 d and clear taxon-specific lifespans ($F_{20,73} = 41.97$, $P < 10^{-15}$). These results suggest that increases in the net population growth rate over time ($k < 1$) resulted in a substantial, but variable, extension of lifespan across phylogenetically diverse taxa. Such findings have the potential to inform biospherics research, which focuses on the dynamics of material cycling and energy flow in closed ecosystems (24).

By specifying a lower observational threshold, we were also able to calculate the expected time to extinction for energy-limited populations (*Materials and Methods* and *SI Appendix*). For the majority of taxa, T_{ext} ranged from 10^0 to 10^2 y, with *Bacillus* being an extreme case with a T_{ext} of $\sim 10^5$ y (Fig. 2*D*). While the timescales of these estimates extend far beyond what can be observed, they provide valuable information that is otherwise challenging to obtain. For example, estimates of $\bar{T}_d$ can inform ecological and evolutionary models that consider long-lived individuals with low metabolic activities (seed banks) (17, 21, 23). Given that T_{ext} can be viewed as the maximum lifespan of a microbial cell since, by definition, extinction occurs when the last individual has died, we can compare our estimates to values reported for other groups of organisms. For example, the maximum lifespan of vertebrates is between $\sim 10^{0.5}$ and $10^{1.7}$ y (14, 53), a range that is nested within that of bacterial lifespans. Our findings are also on par with microbial T_{ext} inferred from phylogenetic analyses, where the range of T_{ext} for birds was nested within the range of bacteria (54).

To further investigate the limits of longevity among diverse taxa, we compared our estimates of T_{ext} to those of seeds, adaptive structures that allow many plants to survive through unfavorable conditions. Typically, plant biologists report the longevity of seeds based on their half-life ($T_{1/2}$), a quantity that can readily be derived from our survival analyses. We estimated that the half-life of an energy-limited bacterium is $\sim 10^{-4}$ to 10^{-2} y. This range is lower than $T_{1/2}$ values reported for 195 angiosperm species ($\sim 10^{-2}$ to $10^{-0.5}$ y) (55), suggesting that the lifespan of a bacterial cell is shorter than that of a typical plant seed. An exception to this generalization is *Bacillus* with an estimated $T_{1/2} \sim 10^{1.4}$ y. This estimate is two orders of magnitude greater than the longest reported half-life of a seed at $\sim 10^{-0.64}$ y and is comparable to the $T_{1/2}$ of seeds maintained in cold storage for the express purpose of life extension (56).

Of the taxa included in our study, *Bacillus* was an outlier in terms of its longevity. It would seem reasonable to attribute its T_{ext} to its ability to form protective endospores, which are some of the most biologically inert forms of life. Even though its values of $N \cdot d_0$ and k do not deviate from the relationship observed among all other taxa (Fig. 2*A*), this consistency could arise if a large portion of the *Bacillus* populations remained in a vegetative state instead of forming endospores ($\sim 70\%$ vegetative cells) (57, 58). In any case, the degree to which endospore formation affects $\bar{T}_d$ and T_{ext} remains unknown. To address this, we constructed a *Bacillus* mutant strain with a deletion of *spoIIE*, a gene that is essential for the formation of endospores. We then conducted an 80-d survivorship experiment with replicate populations of the non–spore-forming mutant (Δ*spoIIE*) and the spore-forming wild type under energy-limited conditions (*SI Appendix*). Both strains exhibited qualitatively similar survival curves, although k was consistently higher for Δ*spoIIE*. Despite the similarity in shape (*SI Appendix*, Fig. S11), the disruption of endospore formation had a strong effect on longevity, reducing $\bar{T}_d$ by 95% and T_{ext} by 98%. Nevertheless, the longevity of Δ*spoIIE* remained high in comparison to other taxa, suggesting that this singular, yet complex, trait was not solely responsible for the longevity of *Bacillus*. Instead, our data suggest that necromass recycling, and perhaps other persistence strategies, contribute to the exceptional longevity of *Bacillus* and its close relatives in energy-limited environments.

Evolutionary Dynamics over 1,000 d. While the number of birth events was low, we investigated evolutionary dynamics from pooled population sequencing. The distribution of mutation frequencies (site frequency spectra) shared a qualitatively similar form across taxa (*SI Appendix*, Fig. S12), consistent with the similar population dynamics that arose across taxa under energy limitation. Indeed, summary statistics revealed that site frequency spectra were highly skewed, such that the difference between the mean number of pairwise differences and the

MICROBIOLOGY

number of segregating sites (Tajima's D, D_T) was greater than zero for all examined taxa (*SI Appendix*, Fig. S13). This pattern is consistent with strong bottlenecking events that accompany a rapid reduction in population size. Indeed, k was marginally correlated with D_T ($\beta_1 = -3.10$, $P = 0.052$), suggesting that the observed values of D_T were driven in part by the demographic history of the system (*SI Appendix*, Fig. S14). However, since all replicates of a given taxon started from a single clone and very little standing genetic variation was shared across taxa, there was initially very little diversity that could undergo a bottleneck during the initial reduction in population size. This seemingly contradictive result can be resolved by considering an alternative demographic model, one where mutations initially increased in frequency, only to contract once necromass was depleted.

Despite the strong bottlenecking that likely occurred due to the rapid decline in population size early in our experiment, there was evidence that natural selection operated over the course of 1,000 d. The ratio of genome-wide nonsynonymous to synonymous polymorphic mutations (pN/pS) was less than 1 for the majority of taxa (Fig. 3), a signal of purifying selection that has been found in microbial populations in the deep biosphere (59, 60). We then searched for potential targets of positive selection by identifying the set of genes that acquired more nonsynonymous mutations than expected by chance. We found that nonsynonymous mutations were nonrandomly distributed across genes in all taxa examined, a potential signal of adaptive evolution (Dataset S2 and *SI Appendix*, Fig. S15). By mapping genes to their higher-level functions, we identified cellular features that contributed to adaptation across multiple taxa, suggestive of convergent evolution. Three pathways were enriched for nonsynonymous mutations in two out of seven taxa: lysine biosynthesis (M00016), pyrimidine biosynthesis (M00053), and branched-chain amino acid transport (M00237). The nonsynonymous mutations acquired in these pathways did not introduce stop codons. Rather, the missense mutations point to pathways that likely contributed to adaptation through modification and refinement, rather than loss of function. For example, the enrichment of lysine and pyrimidine biosynthesis pathways may be involved in more efficient necromass uptake, whereas the enrichment of transporters has previously been documented in populations of starving bacteria (36, 38, 61). While the lack of fixation events was convenient for making demographic inference, it ultimately limits our ability to make concrete claims about the contribution of mutations toward adaptation under energy limitation.

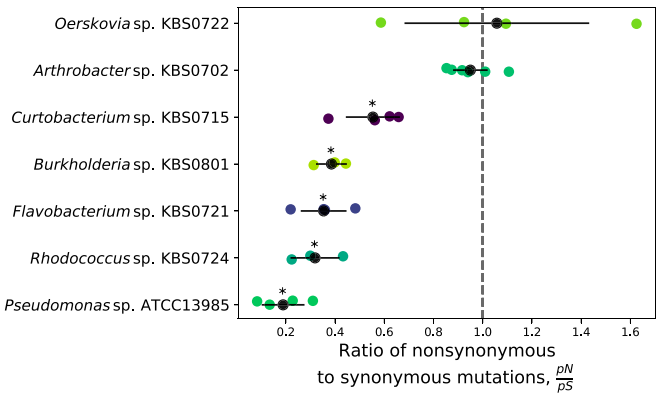

Fig. 3. The ratio of nonsynonymous to synonymous mutations (pN/pS) within each taxon provides evidence for purifying selection under extreme energy limitation. The expected value in the absence of positive or purifying selection is represented by a dashed gray vertical line. The solid black symbol represents the mean within a given taxon across replicate populations, and the black bars represent twice the SE. Asterisks indicate that the mean is significantly less than 1 according to a left-tailed one-sided t test after false discovery rate correction.

Conclusion

In many habitats, the residence time of resources and individuals is long enough that they approach the limit of an effectively closed state. Under such conditions, metabolism and demography are governed by the internal dynamics of the system. By tracking replicate populations of energy-limited bacteria for an extended period of time under highly controlled conditions, we demonstrated that the turnover of dead cells fueled the population dynamics of diverse taxa and held important consequences for persistence and longevity. Bacterial cells survived for $\sim 10^0$ to 10^3 d in the absence of an external resource supply, contributing to a population-level extinction timescale of $\sim 10^0$ to 10^5 y. While bacteria have some of the shortest generation times among autonomous self-replicating organisms, at the same time, we find that their lifespans are comparable to some of the longest-lived plants and animals on the planet. Necromass recycling not only contributed to the maintenance of energy-limited cells but also allowed them to reproduce and evolve through natural selection. We hypothesize that necromass recycling has likely played a role in shaping the historical and ongoing dynamics of natural populations in effectively closed ecosystems that occupy vast expanses of Earth.

Materials and Methods

Constructing Survival Curves. We used a well-characterized collection of 21 bacterial taxa, the majority of which were isolated from soil ecosystems. The collection included representatives from four phyla, seven classes, nine orders, and 16 families and genera (*SI Appendix*, Table S1) that exhibited variation in a suite of functional traits, including biofilm production, motility, desiccation tolerance, maximum growth rate, and respiration (52).

Before initiating the experiment, we inoculated single colony isolates of each taxon into 50 mL Erlenmeyer flasks containing 20 mL of R2B medium. The flasks were incubated at 25 °C and shaken at 150 rpm. Before reaching stationary phase, cultures were split into 50 mL Falcon tubes and then pelleted at 4,500 rpm. We discarded the supernatant and washed the cells five times with pH 7.1 phosphate buffered saline (PBS) to remove residual medium. We began the survival-curve experiment by dispensing washed cells from each taxon into replicate (n = 4 to 8) 50 mL Falcon tubes containing 25 mL of buffered PBS. The populations were maintained in the dark at 25 °C. We tracked cell densities over time by sampling 10 to 100 μL from each population in a HEPA-equipped fume hood to reduce the risk of contamination. Each sample removed 0.2% of the initial volume. By the end of the experiment, the cumulative sampling amounted to 12% of the initial volume, which led to a modest increase (6%) in the headspace. With each sample, we plated dilutions onto R2A plates and counted the number of CFUs. For most taxa, colonies formed within $<$ 48 h, but we tracked plates for up to 2 wk to allow for the emergence of slow-growing individuals. The experiment was run until day 1,000 or until the population went extinct.

Performing Survival Analysis. We statistically modeled the survival of each population over time using the Weibull distribution:

$$S(t) = \exp\left\{-(d_0 \cdot t)^k\right\}, \quad [1]$$

where d_0 is a scale parameter that represents the initial per-capita death rate, k is a shape parameter that describes how the death rate of the system changes over time, and $S(t)$ is the proportion of surviving individuals at time t. Because all populations were in environments with no exogenous resource supply, we interpret initial changes in $N(t)$ to be the result of death events. We compared models ($k = 1$ vs. $k \neq 1$) using the form of the likelihood ratio test provided by Wilks' theorem. Using the estimated Weibull parameters, we calculated the mean time to death (lifespan) of a cell as $T_d = d_0^{-1}\Gamma(1 + 1/k)$, where Γ is the gamma function. The statistical relationship between k and $d_0 \cdot N(0)$ was examined using a mixed-effects linear model via the lmer function (*SI Appendix*) (62). We estimated the marginal coefficient of determination r^2_m using the r.squaredGLMM function from the MuMIn package (63). We estimated the confidence hull with a semiparametric bootstrapping approach using the bootMer function from lmer and

phylogenetic linear regression using phylolm (64). All survival analyses were conducted in R v3.5.0 (65).

Necromass Recycling Model. To explore potential mechanisms underlying the observed survival curves, we examined the dynamics of a system where viable cells (N) die at an initial death rate (d_0) and enter a pool of dead cells (N_d) (66). In this model, dead cells decay into a necromass resource pool (R) at rate (δ) with a given amount of resources per cell (c). Viable cells consume necromass according to Monod kinetics, where $V_{\max}$ is the maximum uptake rate of necromass and K_R is the half-velocity constant. Together, we used the following system of equations to model the change in net population growth rate (m) when maintenance energy costs can be met via the consumption of necromass:

$$\frac{\partial N}{\partial t} = N\left(\frac{1}{m}\frac{V_{\max}R}{K_R+R} - d_0\right), \quad [2a]$$

$$\frac{\partial N_d}{\partial t} = d_0 N - \delta N_d, \quad [2b]$$

$$\frac{\partial R}{\partial t} = c d_0 N_d - N\frac{V_{\max}R}{K_R+R}. \quad [2c]$$

Mutation Calling. To characterize the molecular evolution of bacteria under extreme energy limitation, we performed pooled population sequencing on all replicate populations with sufficient biomass after 1,000 d. We concentrated biomass using MilliporeSigmaAmiconUltra Centrifugal Filter Units. The resulting pellets were resuspended in 1 mL of PBS, centrifuged, and decanted before DNA was extracted using a MoBio UltraClean Microbial DNA Isolation Kit. We prepared libraries using the NEXTflexRapid DNA-Seq Kit (Bioo Scientific) and conducted paired-end sequencing with an Illumina NextSeq 500 High Output for 150 cycles. Raw reads were cleaned and trimmed using cutadapt (67). Mutations were then mapped to hybrid de novo assembled Nanopore and Illumina genomes (see *SI Appendix* for additional details) and called with breseq v0.32.0 (68). We examined mutations in taxa with at least three replicates with a minimum mean genome-wide coverage of 50. Genome-wide likelihood ratios, pN/pS, and gene-specific multiplicity scores were calculated using publicly licensed code (69). We tested whether pN/pS was less than 1 in each taxon using a left-tailed one-sided t test and corrected for multiple testing using the Benjamini–Hochberg procedure from statsmodels (70). The same test was used to determine whether Tajima's D D_T was greater than 1 (*SI Appendix*). Additional information on genetic diversity calculations can be found in *SI Appendix*.

Data Availability. We used open-source computing code and custom scripts to complete our analyses. Raw reads used for assembly are available on the Sequence Read Archive, and assemblies are available through the National Center for Biotechnology Information, with accession numbers listed in Dataset S4. The raw reads from evolved lines are available on SRA (BioProjects PRJNA561216, PRJNA539822, PRJNA373913, PRJNA373912, and PRJNA370526) (71–75). All remaining data are available on Zenodo (doi: 10.5281/zenodo.4458917) (76). All analyses can be reproduced or modified for further exploration using code on GitHub: https://github.com/LennonLab/LTDE.

ACKNOWLEDGMENTS. We acknowledge the Indiana University Bloomington Center for Genomics and Bioinformatics and the University of New Hampshire Hubbard Center for Genome Studies for sequencing support. The research was supported by the NSF (DEB-1442246 and DEB-1934554 to J.T.L.), the US Army Research Office Grant W911NF-14-1-0411 (J.T.L.), and NASA (80NSSC20K0618 to J.T.L.). Genome assembly and mutation calling was made possible by the Lilly Endowment, Inc., through its support for the Indiana University Pervasive Technology Institute; the National Science Foundation under Grant CNS-0521433; and Shared University Research grants from IBM, Inc., to Indiana University.

1. R. J. Parkes *et al*., Deep bacterial biosphere in Pacific Ocean sediments. *Nature* **371**, 410–413 (1994).
2. W. B. Whitman, D. C. Coleman, W. J. Wiebe, Prokaryotes: The unseen majority. *Proc. Natl. Acad. Sci. U.S.A.* **95**, 6578–6583 (1998). https://www.pnas.org/content/95/12/6578
3. M. A. Lever *et al*., Life under extreme energy limitation: A synthesis of laboratory- and field-based investigations. *FEMS Microbiol. Rev.* **39**, 688–728 (2015).
4. N. Merino *et al*., Living at the extremes: Extremophiles and the limits of life in a planetary context. *Front. Microbiol.* **10**, 780 (2019).
5. L. Wörmer *et al*., Microbial dormancy in the marine subsurface: Global endospore abundance and response to burial. *Sci. Adv.* **5**, eaav1024 (2019).
6. R. Y. Morita, Bioavailability of energy and its relationship to growth and starvation survival in nature. *Can. J. Microbiol.* **34**, 436–441 (1988).
7. Y. Morita, *Bacteria in Oligotrophic Environments: Starvation-Survival Lifestyle* (Chapman Hall, New York. 1997).
8. A. Maitra, K. A. Dill, Bacterial growth laws reflect the evolutionary importance of energy efficiency. *Proc. Natl. Acad. Sci. U.S.A.* **112**, 406–411 (2015) https://www.pnas.org/content/112/2/406.
9. D. E. LaRowe, J. P. Amend, Power limits for microbial life. *Front. Microbiol.* **6**, 718 (2015).
10. J. Kallmeyer, R. Pockalny, R. R. Adhikari, D. C. Smith, S. D'Hondt, Global distribution of microbial abundance and biomass in subseafloor sediment. *Proc. Natl. Acad. Sci. U.S.A.* **109**, 16213–16216 (2012). https://www.pnas.org/content/109/40/16213.
11. D. E. Graham *et al*., Microbes in thawing permafrost: The unknown variable in the climate change equation. *The ISME J.* **6**, 709–712 (2012).
12. M. Schostag *et al*., Bacterial and protozoan dynamics upon thawing and freezing of an active layer permafrost soil. *The ISME J.* **13**, 1345–1359 (2019).
13. H. P. Browne, B. Anne Neville, S. C. Forster, T. D. Lawley. Transmission of the gut microbiota: Spreading of health. *Nat. Rev. Microbiol.* **15**, 531–543 (2017). https://www.ncbi.nlm.nih.gov/pmc/articles/PMC5837012/
14. R. Z. Moger-Reischer, J. T. Lennon, Microbial ageing and longevity. *Nat. Rev. Microbiol.* **17**, 679–690 (2019).
15. P. Setlow, Spore germination. *Curr. Opin. Microbiol.* **6**, 550–556 (2003).
16. J. D. Oliver, The viable but nonculturable state in bacteria. *J. Microbiol. (Seoul, Koea)* **43**, 93–100 (2005).
17. J. T. Lennon, S. E. Jones, Microbial seed banks: The ecological and evolutionary implications of dormancy. *Nat. Rev. Microbiol.* **9**, 119–130 (2011).
18. W. L. Nicholson, N. Munakata, G. Horneck, H. J. Melosh, P. Setlow, Resistance of Bacillus endospores to extreme terrestrial and extraterrestrial environments. *Microbiol. Mol. Biol. Rev.* **64**, 548–572 (2000).
19. R. Moeller, G. Reitz, Z. Li, S. Klein, W. L. Nicholson, Multifactorial resistance of Bacillus subtilis spores to high-energy proton radiation: Role of spore structural components and the homologous recombination and non-homologous end joining DNA repair pathways. *Astrobiology* **12**, 1069–1077 (2012).
20. C. I. Abreu, J. Friedman, V. L. A. Woltz, J. Gore, Mortality causes universal changes in microbial community composition. *Nat. Commun.* **10**, 1–9 (2019).
21. J. Blath, A. G. Casanova, B. Eldon, N. Kurt, M. Wilke-Berenguer, Genetic variability under the seedbank coalescent. *Genetics* **200**, 921–934 (2015).
22. I. Levin-Reisman *et al*., Antibiotic tolerance facilitates the evolution of resistance. *Science (New York, N.Y.)* **355**, 826–830 (2017).
23. W. R. Shoemaker, J. T. Lennon, Evolution with a seed bank: The population genetic consequences of microbial dormancy. *Evol. Appl.* **11**, 60–75 (2018).
24. M. C. Rillig, J. Antonovics, Microbial biospherics: The experimental study of ecosystem function and evolution. *Proc. Natl. Acad. Sci. U.S.A.* **116**, 11093–11098 (2019).
25. W. P. Dietrich, T. Dunne, Sediment budget for a small catchment in a mountainous terrain. *Z. Geomorphol.* **29**, 191–206 (1978).
26. R. E. Bell *et al*., Origin and fate of Lake Vostok water frozen to the base of the East Antarctic ice sheet. *Nature* **416**, 307–310 (2002).
27. A. D. Friend *et al*., Carbon residence time dominates uncertainty in terrestrial vegetation responses to future climate and atmospheric CO2. *Proc. Natl. Acad. Sci. U.S.A.* **111**, 3280–3285 (2014).
28. K. J. Locey, J. T. Lennon, A residence time theory for biodiversity. *Am. Nat.* **194**, 59–72 (2019).
29. W. Wieser, Cost of growth in cells and organisms: General rules and comparative aspects. *Biol. Rev. Camb. Philos. Soc.* **69**, 1–33 (1994).
30. D. E. Rozen, N. Philippe, J. Arjan de Visser, R. E. Lenski, D. Schneider, Death and cannibalism in a seasonal environment facilitate bacterial coexistence. *Ecol. Lett.* **12**, 34–44 (2009).
31. C. P. Kempes *et al*., Drivers of bacterial maintenance and minimal energy requirements. *Front. Microbiol.*, 10.3389/fmicb.2017.00031 (2017).
32. J. A. Bradley, J. P. Amend, D. E. LaRowe, Necromass as a limited source of energy for microorganisms in marine sediments. *J. Geophys. Res. Biogeosci.* **123**, 577–590 (2018).
33. S. J. Schink, E. Biselli, C. Ammar, U. Gerland, Death rate of E. coli during starvation is set by maintenance cost and biomass recycling. *Cell Syst.* **9**, 64–73.e3 (2019).
34. F. J. Ryan, Bacterial mutation in a stationary phase and the question of cell turnover. *J. Gen. Microbiol.* **21**, 530–549 (1959).
35. S. E. Finkel, R. Kolter, Evolution of microbial diversity during prolonged starvation. *Proc. Natl. Acad. Sci. U.S.A.* **96**, 4023–4027 (1999).
36. S. E. Finkel, Long-term survival during stationary phase: Evolution and the GASP phenotype. *Nat. Rev. Microbiol.* **4**, 113–120 (2006).
37. S. Avrani, E. Bolotin, S. Katz, R. Hershberg, Rapid genetic adaptation during the first four months of survival under resource exhaustion. *Mol. Biol. Evol.* **34**, 1758–1769 (2017).
38. S. Katz *et al*., Dynamics of adaptation during three years of evolution under long-term stationary phase. *Mol. Biol. Evol.* **38**, 2778–2790 (2021).
39. J. Gross, S. Avrani, S. Katz, S. Hilau, R. Hershberg, Culture volume influences the dynamics of adaptation under long-term stationary phase. *Genome Biol. Evol.* **12**, 2292–2301 (2020).
40. T. Aouizerat *et al*., Eukaryotic adaptation to years-long starvation resembles that of bacteria. *iScience* **19**, 545–558 (2019).
41. B. A. Lomstein, A. T. Langerhuus, S. D'Hondt, B. B. Jørgensen, A. J. Spivack, Endospore abundance, microbial growth and necromass turnover in deep sub-seafloor sediment. *Nature* **484**, 101–104 (2012).

42. E. D. Becraft *et al*., Evolutionary stasis of a deep subsurface microbial lineage. *ISME J.* 1–13 (2021).
43. A. Papoulis, S. Unnikrishna Pillai, *Probability, Random Variables, and Stochastic Processes* (McGraw-Hill, ed. 4, 2009).
44. C.-E. A. Winslow, B. Cohen, Relative ability of B. coli and B. aerogenes types in water. *J. Infect. Dis.* **23**, 82–89 (1918).
45. B. Cohen, The resistance of the Glanders Bacillus to calcium hypochlorite. *J. Infect. Dis.* **24**, 51–55 (1919).
46. K. Mather, The analysis of extinction time data in bioassay. *Biometrics* **5**, 127–143 (1949).
47. R. E. Ricklefs, Insights from comparative analyses of aging in birds and mammals. *Aging Cell* **9**, 273–284 (2010).
48. C. Pin, J. Baranyi, Single-cell and population lag times as a function of cell age. *Appl. Environ. Microbiol.* **74**, 2534–2536 (2008).
49. I. Levin-Reisman *et al*., Automated imaging with ScanLag reveals previously undetectable bacterial growth phenotypes. *Nat. Methods* **7**, 737–739 (2010).
50. Y. Himeoka, K. Kaneko, Theory for transitions between exponential and stationary phases: Universal laws for lag time. *Phys. Rev. X* **7**, 021049 (2017).
51. C. T. Brown, M. R. Olm, B. C. Thomas, J. F. Banfield, Measurement of bacterial replication rates in microbial communities. *Nat. Biotechnol.* **34**, 1256–1263 (2016).
52. J. T. Lennon, Z. T. Aanderud, B. K. Lehmkuhl, D. R. Schoolmaster, Mapping the niche space of soil microorganisms using taxonomy and traits. *Ecology* **93**, 1867–1879 (2012).
53. K. Healy *et al*., Ecology and mode-of-life explain lifespan variation in birds and mammals. *Proc. R. Soc. B Biol. Sci.* **281**, 20140298 (2014). https://royalsocietypublishing.org/doi/full/10.1098/rspb.2014.0298
54. S. Louca *et al*., Bacterial diversification through geological time. *Nat. Ecol. Evol.* **2**, 1458–1467 (2018).
55. R. J. Probert, M. I. Daws, F. R. Hay, Ecological correlates of ex situ seed longevity: A comparative study on 195 species. *Ann. Bot.* **104**, 57–69 (2009).
56. L. Colville, H. W. Pritchard, Seed life span and food security. *New Phytol.* **224**, 557–562 (2019).
57. M. Borisova *et al*., Peptidoglycan recycling in gram-positive bacteria is crucial for survival in stationary phase. *mBio* **7**, e00923–16 (2016).
58. D. A. Gray *et al*., Extreme slow growth as alternative strategy to survive deep starvation in bacteria. *Nat. Commun.* **10**, 1–12 (2019).
59. J. F. Biddle *et al*., Prospects for the study of evolution in the deep biosphere. *Front. Microbiol.* **2**, 285 (2012).
60. P. Starnawski *et al*., Microbial community assembly and evolution in subseafloor sediment. *Proc. Nat. Acad. Sci. U.S.A.* **114**, 2940–2945 (2017).
61. M. N. L. Juana, A. Tormo, E. Martínez-García, Stationary phase in gram-negative bacteria. *FEMS Microbiol. Rev.* **34**, 476–495 (2010).
62. D. Bates, M. Mächler, Ben Bolker, and Steve Walker. Fitting linear mixed-effects models using lme4. *J. Stat. Softw.* **67**, 1–48 (2015).
63. K. Barton, Mu-MIn: Multi-model inference. R Package Version 0.12.2/r18. (2009).
64. L. S. T. Ho, C. Ané, A linear-time algorithm for Gaussian and non-Gaussian trait evolution models. *Syst. Biol.* **63**, 397–408 (2014).
65. R Core Team, *R: A Language and Environment for Statistical Computing*. (R Foundation for Statistical Computing, Vienna, Austria, 2018).
66. S. Takano, B. J. Pawlowska, I. Gudelj, T. Yomo, S. Tsuru, Density-dependent recycling promotes the long-term survival of bacterial populations during periods of starvation. *mBio* **8**, e02336–16 (2017).
67. M. Martin, Cutadapt removes adapter sequences from high-throughput sequencing reads. *EMBnet.journal* **17**, 10–12 (2011).
68. D. E. Deatherage, J. E. Barrick, Identification of mutations in laboratory-evolved microbes from next-generation sequencing data using breseq. *Methods Mol. Biol. (Clifton, N.J.)* **1151**, 165–188 (2014).
69. B. H. Good, M. J. McDonald, J. E. Barrick, R. E. Lenski, M. M. Desai, The dynamics of molecular evolution over 60,000 generations. *Nature* **551**, 45–50 (2017).
70. S. Seabold, J. Perktold, "Statsmodels: Econometric and statistical modeling with python" in *9th Python in Science Conference* (SciPy, 2010), pp. 92–96.
71. W. R. Shoemaker *et al*., Long-term energy limitation metagenomic sequencing. NCBI. https://www.ncbi.nlm.nih.gov/bioproject/561216. Deposited 20 August 2019.
72. W. R. Shoemaker *et al*., Long-term dormancy experiment. NCBI. https://www.ncbi.nlm.nih.gov/bioproject/539822. Deposited 25 April 2019.
73. W. R. Shoemaker *et al*., Arthrobacter sp. KBS0703 Genome sequencing and assembly. NCBI. https://www.ncbi.nlm.nih.gov/bioproject/373913. Deposited 28 February 2017.
74. W. R. Shoemaker *et al*., Micrococcus sp. KBS0714 genome sequencing. NCBI. https://www.ncbi.nlm.nih.gov/bioproject/373912. Deposited 31 July 2019.
75. W. R. Shoemaker *et al*., Flavobacterium sp. KBS0721 isolate:KBS0721 genome sequencing. NCBI. https://www.ncbi.nlm.nih.gov/bioproject/370526. Deposited 31 July 2019.
76. W. R. Shoemaker *et al*., The Evolution and ecology of energy-limited microbial populations. Zenodo. https://zenodo.org/record/4458917. Deposited 25 January 2021.